Proceedings of the
18th symposium on energy engineering sciences
Argonne National Laboratory, May 2000

OPTIMIZATION OF HEAT TRANSFER EFFECTIVENESS IN HETEROGENEOUS MEDIA

V.S.Travkin, I.Catton and K. Hu
University of California, Los Angeles
Mechanical and Aerospace Engineering Department
Los Angeles, CA 90095-1597

ABSTRACT

Developments of Volume Averaging Theory (VAT) to describe transport phenomena in heterogeneous media are applied to optimization of heat dissipation from a heterogeneous media. The media is an unspecified porous (heterogeneous) layer and the optimization process is accomplished with rigor using the idea of scaled energy transport. The enhancement of heat transport is stated mathematically in a way that the lower scale conventional pin heat transport enhancement and the performance of the total device are incorporated for optimization. The problem is addressed in three steps: 1) solution of a two-temperature problem with inclusion of experimental data correlations, 2) statistical design of experiments (simulating the problem) for problems with many optimization parameters, and 3) optimization of 2D heterogeneous volumetric heat removal by conduction and convective exchange. The analysis distinguishes certain classes of distributed parameter optimization statements whose solutions determine global "in-class" upper limits of heat enhancement (for a given set of physical assumptions).

1. ITRODUCTION

Development of a VAT mathematical basis and models for optimization of a heterogeneous, hierarchical scaled media began with work by Travkin, Gratton and Catton [1] and is followed by a series of papers [2-4] documenting the development of a method that is applicable to a wide variety of transport phenomena ranging from fluid mechanics to crystal photonic band-gap problems [5], clearly demonstrating the interdisciplinary nature the multi-scale VAT description of transport phenomena. The theoretical development of transport phenomena in heterogeneous media with multiple scales has now been brought to the level where a specific application can be chosen for demonstration. The application chosen is enhancement of heat transfer dissipation from a heterogeneous media while minimizing the frictional resistance (a problem of importance to all designers of heat exchangers). This problem has been under investigation for more than 3 decades and in spite of its longevity and importance as a problem, it has not been satisfactorily treated.

A majority of past investigations focused on solutions to a specific optimization task with a very limited number of spatial parameters to be varied, usually a fixed geometric configuration, that they tuned in their search for a maximum level of heat exchange (see, for example, Bejan and co-authors [6,7] and references therein). This approach is a "single-scale" approach yielding an optimum for a certain morphology and flow intensity without giving an explanation for why it was achieved. Without an explanation, there is no guidance on how to change the design to improve its performance. For each new morphology, the experiment, whether real or numerical, needs to be performed again. In the heat exchanger industry there are countless research studies devoted to this problem.

In this work we outline how earlier studies [1-5] can be applied to a practical application. The present treatment of the heat exchange optimization process can be applied to any specific hierarchical heterostructure with the aim to optimize its performance. What has been done is a demonstration of the only heterogeneous media modeling tool that combes both mathematical and morphological descriptions in one problem statement.

2. VAT EQUATIONS IN THE FORM OF CONTROL EQUATIONS

The averaged laminar momentum equation

$$-\frac{\partial}{\partial z}\left\langle m(z)\frac{\partial \theta(z)}{\partial z}\right\rangle + U_{M\,Conv} + U_{M\,Friction} - U_{M\,Drag} = \frac{1}{\varepsilon_f}\frac{\partial \langle m(z)\rangle^{\beta}}{\partial x}; \qquad (1)$$

is "controlled" by the three morphological terms that are defined as the "morpho-convective" fluctuation field distribution based term

$$U_{M\,Conv}(\beta; w\beta; \partial S_w; \phi_f; \phi_s) = \frac{\partial}{\partial z}\left[\langle \beta w\beta\rangle_f\right]; \qquad (2)$$

the interface surface skin friction term

$$U_{MFriction}(U;@S_w;\circ) = \frac{\circ}{\text{¢}} \int_{@S_w} \frac{@U}{@x_i}\,\text{¢}\,ds; \tag{3}$$

and the solid phase drag resistance term

$$U_{MDrag}(p_j;@S_w) = \frac{1}{\%_f\,\text{¢}} \int_{@S_w} p\,ds; \tag{4}$$

where the second left hand side term $@\,\langle \text{¡}\,\tilde{u}\tilde{w}\rangle_f/@z$ presents cross-fluctuations effect. The presence of the vertical velocities $-\tilde{W}$ and $\tilde{W}_f$; or $\tilde{w} = \tilde{W} - \tilde{W}_f$; seen in the first term, do not exist at the macrolevel because z direction momentum transport is only present locally close to obstacles. In traditional (homogeneous) one-scale shape optimization approaches these three terms are not presented (see, for example, Ledezma et al. [7]) and, as a result, optimization methods are very restricted in their value and clearly the macroscopic behavior cannot be related to the bottom scale enhancement.

The laminar fluid energy equation is

$$c_{pf}\%_f\langle m\rangle_i\left(\frac{@\tilde{T}_f}{@x}\right) = k\frac{@}{@x}\left[\frac{@\langle m\rangle_i\tilde{T}_f}{@x}\right] + k\frac{@}{@z}\left[\frac{@\langle m\rangle_i\tilde{T}_f}{@z}\right] +$$

$$+ T_{fMConvX} + T_{fMConvZ} + T_{fMSurfX} + T_{fMSurfZ} + T_{fMExchange}: \tag{5}$$

with the five additional control terms being

$$T_{fMConvX}\left(\tilde{p}_f;\tilde{u};\text{¢}_f;\text{¢}_s\right) = c_{pf}\%_f\frac{@}{@x}\left[\langle m\rangle_i\left(\tilde{p}_f\tilde{u}\right)_f\right]; \tag{6}$$

$$T_{fMConvZ}\left(\tilde{p}_f;\tilde{w};\text{¢}_f;\text{¢}_s\right) = c_{pf}\%_f\frac{@}{@z}\left[\langle m\rangle_i\left(\tilde{p}_f\tilde{w}\right)_f\right]; \tag{7}$$

$$T_{fMSurfX}(k;T_f;@S_w) = k\frac{@}{@x}\left[\frac{1}{\text{¢}}\int_{@S_w} T_f\,ds\right]; \tag{8}$$

$$T_{fMSurfZ}(k;T_f;@S_w) = k\frac{@}{@z}\left[\frac{1}{\text{¢}}\int_{@S_w} T_f\,ds\right]; \tag{9}$$

$$T_{fMExchange}(k;T_f;@S_w) = \frac{k}{\text{¢}}\int_{@S_w}\frac{@T_f}{@x_i}\,\text{¢}\,ds; \tag{10}$$

Finally, the solid phase energy equation has the similar additional terms. In the turbulent regime, the momentum, fluid energy and solid energy equations are similar to what are shown but with an increased number of control terms and more complexity. They are not reproduced here and can be found in [2,4,5]. Some discussion about how they will be dealt with is found in the final section of this paper.

The control equations are made general by non-dimensionalization with the following scaling, see Fig. 1,

$$S_w = S_w^{\text{¤}}S_{wm};\; z = z_m z^{\text{¤}};\; z_m = \frac{4m_0}{S_{wm}};\; \tilde{U} = u_m u^{\text{¤}};\; T_m = \frac{z_m Q_0}{K_{Tm}};\; \circ = z_m u_m \circ^{\text{¤}};\; \langle m(z)\rangle_i = m_0\langle m^{\text{¤}}\rangle_i;$$

$$c_d = C_d^{\text{¤}}c_{dm};\; c_{dm} = \frac{2u_m^2}{u_0^2};\; \frac{1}{\%_f}\frac{d\langle p\rangle_f}{dx} = \text{¡}\,\frac{u_m^2}{z_m};\; k_{fm} = z_m u_m c_{pf}\%_f;\; k_f = k_f^{\text{¤}}z_m u_m c_{pf}\%_f;\; k_s = k_s^{\text{¤}}z_m u_m c_p\%_s:$$

The parameters resulting for laminar flow through a morphology that is constant normal to the flow direction are given in the following table with there possible ranges. These parameters are at the discretion of the designer of a heat transfer device and can be used for optimization.

Name	variable	min	max	Physical meaning of the parameter
$\mathbf{L}_{3N}$	$= Re_{mf} c_{dm} C_d^{\alpha} S_w^{\alpha}$	10^{-5}	$5 \pounds 10^{7}$	influence of media resistance to flow
L_{M4N}	$= Re_{mf}\ (1=m_0)$	10^{-3}	10^{5}	media Reynolds number
L_{P5}	$= \frac{1}{Pe_m} = \frac{z_m u_m}{a_f}$	2:1	$2 \pounds 10^{7}$	Peclet number, $Pe = (\frac{4m_0}{S_{mw}}(\ddot{\imath}\ \frac{z_m}{½_f}\frac{d<p>_f}{dx})^{1=2})=a_f$
L_{P6}	$= \mathbb{R}_L^{\alpha} S_w^{\alpha} = \frac{\mathbb{R}_L S_w}{\mathbb{R}_{Lm} S_{Lm}}$	1:0	10^{8}	heat exchange between phases, $\mathbb{R}_L^{\alpha} S_w^{\alpha} = \frac{\mathbb{R}_L S_w}{u_m c_p ½_f S_{wm}}$
$\mathbf{L}_{P7N}$	$= \frac{Pe_m}{A_k(L_{M4}\ddot{\imath}\ 1)} \mathbb{R}_L^{\alpha} S_w^{\alpha}$	0	10^{20}	parameter from solid phase energy equation
L_{B8}	$= \frac{A_k}{Pe_m} = A_k L_{p5}$	10^{-3}	10^{12}	parameter from II kind BC, see [8]

There are **six** nondimensional control parameters and functions, denoted Medium Specific Control Functions (MSCF),that control the heat and momentum transport in the selected porous medium and that can be modified to optimize the performance. The two terms with the broadest range also have the greatest influence on the outcome. If the morphology functions denoting porosity, $\hbar m(z)i$; and specific surface area, $S_w(z)$;are coordinate specific, then the equations and and parameters sets are different yielding **eight** control parameters instead of six. A similar exersize for turbulent flow with $\hbar mi = const;\ S_w = const$ will yield **eight** optimization parameters.

3. PRELIMINARY OPTIMIZATION METHODS

Some simulation results using VAT based transport and closure models for flow in a channel with rib roughened walls, spherical beads, round tube banks and square tube banks yielded optimal configurations. The morphology models used in the numerical simulations are shown in Fig.1 (see [9]).

The parameters chosen for simulation of flow across spherical beads in a channel were pitch, $P = 20mm$; channel height, $2h = 200mm$;. and bead diameter, $0{:}001mm < d_p < 20mm$. When the diameter of the beads is large, the disturbance of the porosity across the channel is large and the flow resistance plays an important role. As a result the disturbance of the velocity profile is large. When the porosity approaches unity the disturbance of velocity profile disappears and the velocity distribution approaches the theoretical distribution. From a physical viewpoint, this is obvious. When there are no obstacles in the channel, the channel the results are consistent with the theoretical results in contrast with some other models.

The pitch chosen of the rods are the same as those for the beads. The height of the rods is the same as channel height. . The porosity is easily varied from 0 to 1:0: by ranging the tube dimension, d_p. The friction factor for flow across square tube banks and circular tube banks were developed from the micromodeling results of Souto & Moyne [10] and Watanabe [11] respectively.

By application of SVAT closure models to some general morphology models (orifices and plane slits), in limiting cases, it was demonstrated earlier [1-3,8,9] that both the transport model and the closure scheme are reasonable. At the same time, studying the limiting cases of porosity in the channel highlighted mistakes in other studies. The numerical results demonstrate how the simplest morphological properties of a porous layer such as porosity function and specific surface along with closure models naturally affects the transport features and and that it can be helpful in the development of optimized morphologies.

Fig. 2 shows the dependence of the effectivness number, E_{ff}; on the porosity for different morphologies at different Reynolds numbers. E_{ff} is a combination of the Nusselt number, the friction factor and the pore Reynolds number,

$$E_{ff} = \frac{Nu}{Re_{por} f^{1=3}};\ \text{with}\ Nu = \frac{\mathbb{R} d_{por}}{k_f};\ Re_{por} = \frac{4\hbar mi \mathbb{R}}{^{o} S_w}\ \text{and}\ f = \frac{d_h}{2\%_f \mathbb{R}^2}\left(\frac{P}{L}\right) \tag{11}$$

Fig 2 shows how E_{ff} increases as the porosity of the channel decreases. When the porosity decreases, the beads inside the channel play a more important role in increasing the heat transfer while increasing the flow resistance. (for channel filled with regularly arranged spherical beads, the porosity of the channel has a lower limit of 0.4). Fig. 3 and 4 clearly demonstrates an optimum value of E_{ff} .When the porosity is higher than some critical value, the porous media play a more important role in increasing the heat transfer than in increasing the drag resistance. But when the porosity is too low, the drag resistance will be high and E_{ff} will approach 0 when the porosity approaches 0.

When the problem becomes multi-dimensional, 6D or 8D, according to [12-15], it is convenient to use the statistical design of experiment (DOE) methodology.An optimal response surface was found in two steps. First, numerical simulation was carried out based on statistical selction of the parameter values. Second a statistical analysis of the results was used to develop a response surface. This procedure was implemented using a commercial computer code based on DOE.

When the optimization variable is choosen, in our case E_{ff};the variables are systematically defined, see the table of parameters developed above. Next, the numerical experiment design type is selected,e.g. a classical two level,

mixed level,or nested level. The design type used in this work is the classical two level design. The classical two level designs are based on standard orthogonal arrays that contain two levels for each experimental variable. It enables estimation of the effects of some or all terms in a second order model of the general form

$$E_{ff} = a_0 + a_1X_1 + a_2X_2 + \cdots + a_nX_n + a_{11}X_1^2 + a_{12}X_1X_2 + \cdots + a_{n;n\,i\,1}X_nX_{n\,i\,1} + a_{nn}X_n^2$$

The independent variables $X_{1;}X_{2;}\cdots X_n$ are the design variables $L_{3N}\cdots L_{B8}$. Based on the design type and design variables, experiment design options will be created. Each option is a set of input parameters for numerical simulation.Description of what was done to obtain the "experimental results" from the VAT based laminar or turbulent transport equations for flow in a specific porous media is decribed elsewhere (see [8,9]).

After numerical simulation, the numerical results are rigorously analyzed using statistical analysis tools and graphics tools. These tools include nonlinear response/error analysis, experimental error analysis, regression analysis, residuals analysis, two dimensional graphing, three dimensional response surface graphing, and multi response optimization. One of the response surfaces of our study is shown in Fig. 5. The three dimensional figure shows E_{ff} as a function of two variables L_{P2} and L_{M4} (these were chosen for simplicity from the eight independent varables analysed) when the other variables are fixed. Although limited by the range of the variables, the optimum point is shown on the figure.and the trend of the response surface clearly shown in Fig. 5.

4. TWO- AND THREE-SCALE OPTIMIZATION STUDY

Closure of the turbulent regime VAT equations for a porous flat channel also requires closure of additional terms in the governing equations. This is done (as for laminar regime) using Direct Numerical Modeling (DNM). The four terms arrising in the momentum equation are

$$\frac{@}{@z}\left(\mu_m\frac{@\overline{u}}{@z}\right)_f\,;\ \frac{@}{@z}\left(\rho_f\overline{w}\right)_f\,;\ \frac{1}{¢\,\text{-}}\int_{@S_w}(K_m+\text{º})\frac{@\overline{U}}{@x_i}¢\,d\vec{s};\ \frac{1}{\%_f\,¢\,\text{-}}\int_{@S_w}\overline{p}\,d\vec{s}; \tag{12}$$

the seven terms in the fluid temperature equation

$$\frac{@}{@x}\left(k_T\frac{@\overline{T}_f}{@x}\right)_f\,;\ \frac{@}{@z}\left(k_T\frac{@\overline{T}_f}{@z}\right)_f\,;\ c_{pf}\%_f\frac{@}{@x}\left(\langle m\rangle_i\overline{T}_f\overline{u}\right)_f\,;\ c_{pf}\%_f\frac{@}{@z}\left(\langle m\rangle_i\overline{T}_f\overline{w}\right)_f\,; \tag{13}$$

$$\frac{@}{@x}\left[\frac{k_T+k}{¢\,\text{-}}\int_{@S_w}\overline{T}_f\,d\vec{s}\right];\ \frac{@}{@z}\left[\frac{k_T+k}{¢\,\text{-}}\int_{@S_w}\overline{T}_f\,d\vec{s}\right];\ \frac{1}{¢\,\text{-}}\int_{@S_w}(K_T+k)\frac{@\overline{T}_f}{@x_i}¢\,d\vec{s} \tag{14}$$

and five terms in the solid phase temperature equation

$$\frac{@}{@x}\left(k_s\frac{@\overline{T}_s}{@x}\right)_s\,;\ \frac{@}{@z}\left(k_s\frac{@\overline{T}_s}{@z}\right)_s\,;\ \frac{@}{@x}\left[\frac{fK_sg_s}{¢\,\text{-}}\int_{@S_{w12}}T_s\,d\vec{s}_1\right];\ \frac{@}{@z}\left[\frac{fK_sg_s}{¢\,\text{-}}\int_{@S_{w12}}T_s\,d\vec{s}_1\right];\ \frac{1}{¢\,\text{-}}\int_{@S_{w12}}K_{sT}\frac{@T_s}{@x_i}¢\,d\vec{s}_1 \tag{15}$$

The mathematical implementation needed to obtain closure of the momentum resistance terms, for example, for optimization of the morphology of straight rib fins, see Fig. 6a,b; is dictated by the geometry of the fins. For example, if $d\vec{s} = \vec{n}\,ds;\ \vec{n} = (\,\text{¡}\,i;0;0)j_{@S_{wL}}$ and $\vec{n} = (i;0;0)j_{@S_{wR}}$; then the surface integral over the $@S_w$ in each of the intermediate REVs not including portions of the free volume above the fins and those at the bottom of the solid phase of the channel will be, for the x-coordinate frictional resistance component,

$$\frac{1}{¢\,\text{-}}\int_{@S_w}(K_m+\text{º})\,n_i¢\frac{@U_j}{@x_i}ds = \left(\frac{1}{¢\,\text{-}}\int_{@S_w}(K_m+\text{º})\left[n_x\frac{@U}{@x}+n_y\frac{@U}{@y}+n_z\frac{@U}{@z}\right]ds\right)i =$$

$$= \left(\frac{i\,1}{¢\,\text{-}}\int_{z_{kL}}^{z_{(k+1)L}}(K_m+\text{º})\frac{@U}{@x}\Big|_{@S_{wL}}dz + \frac{1}{¢\,\text{-}}\int_{z_{kR}}^{z_{(k+1)R}}(K_m+\text{º})\frac{@U}{@x}\Big|_{@S_{wR}}dz\right)i: \tag{16}$$

The calculation of the form drag portion of resistance loss in momentum VAT equation is done in the same

mode

$$\frac{1}{\%_f\,¢\,-}\int_{@S_w}\bar{p}\,d\vec{s}=\frac{1}{\%_f\,¢\,-}\int_{@S_w}\bar{p}\,\hat{n}\,ds=\left(\frac{i\,1}{\%_f\,¢\,-}\int_{z_{kL}}^{z_{(k+1)L}}\bar{p}j_{@S_{wL}}\,dz\right)i+\left(\frac{1}{\%_f\,¢\,-}\int_{z_{kR}}^{z_{(k+1)R}}\bar{p}j_{@S_{wR}}\,dz\right)i: \quad (17)$$

This is the classical form drag portion of the total kinetic energy loss (shown here only for the x-component). Closure of other terms in the VAT equations are based on the specific two- or three scale morphologies chosen.

Our analysis of many existing morphological solutions has led us to conclude that the scaled hierarchical VAT description gives us the ability to find an optimum morphology that cannot be improved when the selection of fluids and solid phase materials has been made, and the pressure drop through the media is specified. Given these initial conditions (restrictions), it is possible to find a morphology that cannot be improved based on two scale heat transport meaning that there is no other solid phase configuration that can be more efficient than the one that has been found.

5. SUMMARY

In this breif paper we have illustrated a method hierarchical optimization of two- and three scale heat transport in a heterogeneous meda. It is shown how traditional governing equations developed using rigorous VAT methods can be used to optimize surface transport processes in support of heat transport technology.

The difficulty in treating a multiparameter (more than 3) problem, even linear, arewell known to be very difficult to overcome using a parameter sorting process. The combination of VAT based equations and the theory of statistical design to was used to effectively begin treating 6D or 8D optimization volumes.

We have shown how a two scale heterogeneous heat transfer optimization problem can be solved using exact procedures for closure of additional differential and integral VAT terms. This method is shown to be as simple as calculating the appropriate integrals over the morphologies with coordinate surfaces of interfaces pertinent to a morphology of interest. For more complex or even unknown morphologies, as initial spacial morphologies the mathematical methods were outlined in detail. These three tasks were carried out, albeit for some elementary morphologies, for the first time.

6. ACKNOWLEDGMENT

This work was sponsored by the U.S. Department of Energy, Office of Basic Energy Sciences under the Grant DE-FG03-89ER14033 A002.

7. REFERENCES

1. Travkin, V.S., Gratton, L., and Catton, I. (1994), "A Morphological-Approach for Two-Phase Porous Medium-Transport and Optimum Design Applications in Energy Engineering," *Proceedings of the Twelfth Symposium on Energy Engineering Sciences*, Argonne National Laboratory, Conf. -9404137, pp. 48-55.

2. Gratton, L., Travkin, V.S., and Catton, I. (1996), "The Influence of Morphology upon Two- Temperature Statements for Convective Transport in Porous Media," *Journal of Enhanced Heat Transfer*, Vol. 3, No. 2, pp.129-145.

3. Catton, I. and Travkin, V.S. (1997), "Homogeneous and Non-Local Heterogeneous Transport Phenomena with VAT Application Analysis", P*roceedings of the 15th Symposium on Energy Engineering Sciences*, Argonne National Laboratory, Conf. - 9705121, pp. 48-55.

4. Travkin, V.S. and Catton, I., (1998a), "Porous Media Transport Descriptions - Non-Local, Linear and Nonlinear Against Effective Thermal/Fluid Properties", in *Advances in Colloid and Interface Science*, Vol. 76-77, pp. 389-443.

5. V.S.Travkin and I. Catton, (2000), "Transport Phenomena in Heterogeneous Media Based on Volume Averaging Theory", in print *Advances in Heat Transfer*, Vol. 34.

6. Bejan, A. and Morega, A.M. (1993), "Optimal Arrays of Pin Fins and Plate Fins in Laminar Forced Convection," Journal of Heat Transfer, Vol. 115, pp. 75-81.

7. Ledezma, G., Morega, A.M., and Bejan, A. (1996), "Optimal Spacing Between Pin Fins with Impinging Flow," *Journal of Heat Transfer*, Vol. 118, pp. 570-577.

8. Travkin, V.S. and Catton, I. "A Two-Temperature Model for Turbulent Flow and Heat Transfer in a Porous Layer," J. Fluids Eng., 117, 181 (1995).

9. V. S. Travkin, I. Catton,and K. Hu (1998), "Channel Flow In Porous Media In The Limit As Porosity Approaches Unity", in *Proc. ASME HTD-Vol. 361-1*, Vol. 1, pp. 277-284.

10. Souto, H.P.A. and Moyne, C., (1997), "Dispersion in Two-Dimensional Periodic Media. Part II. Dispersion Tensor", *Phys. Fluids*, Vol. 9, No. 8, pp. 2253-2263.

11 Watanabe, H., 1989, Drag coefficient and voidage function on fluid flow through granular packed beds, *International Journal of Engineering Fluid Mechanics*, Vol. 2, No. 1, pp. 93-108.

12. Atwood, C. L. (1969), "Optimal and Efficient Designs of Experiments", *Annals of Mathematical Statistics*, Vol. 40, No. 5, pp. 1570.

13. Box, G. E. P. and Draper, N. R. (1987), *Empirical Model Building and Response Surfaces*, John Wiley & Sons, New York.

14. Diamond, W. J. (1981), *Practical Experiment Designs for Engineers and Scientist*, Wadsworth, Inc.

15. Montgomery, D. C., (1991), *Design and Analysis of Experiments*, 3rd Edition, John Wiley & Sons, New York.

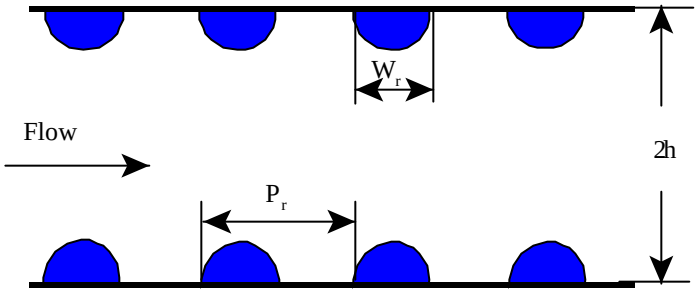

a. Two dimensional semi-cylindrical rib type roughness model

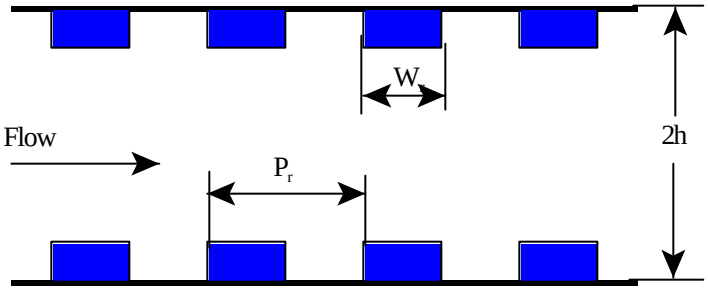

b. Two dimensional rectangular rib type roughness model

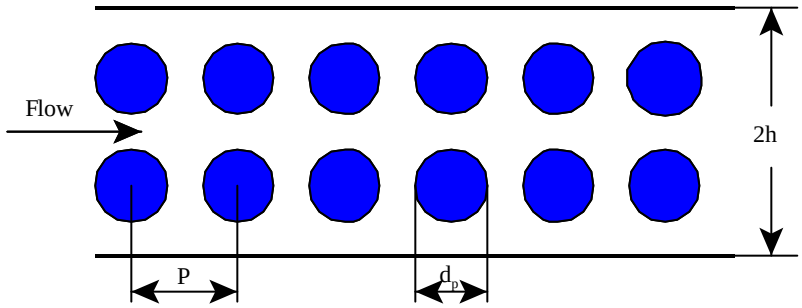

c. Channel flow across the lattice of spherical beads

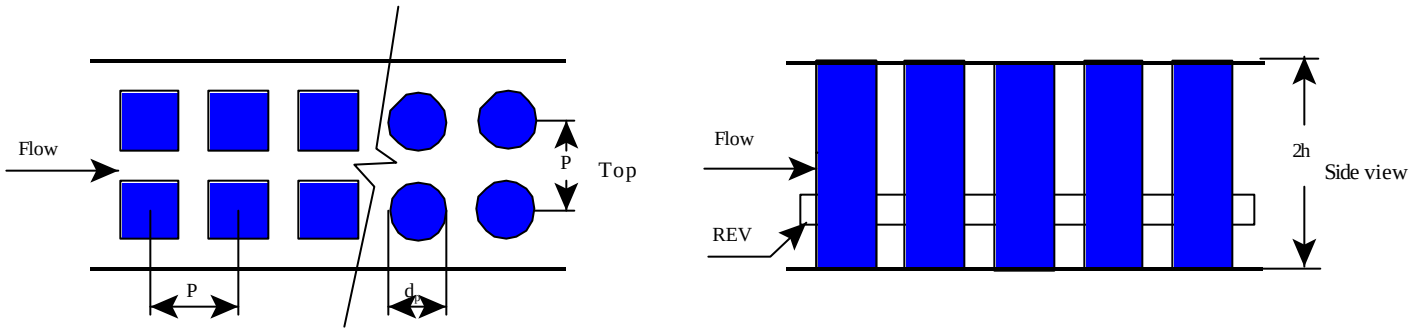

d. Channel flow across rectangular and circular tube banks

Fig. 1 Some channel flow morphologies

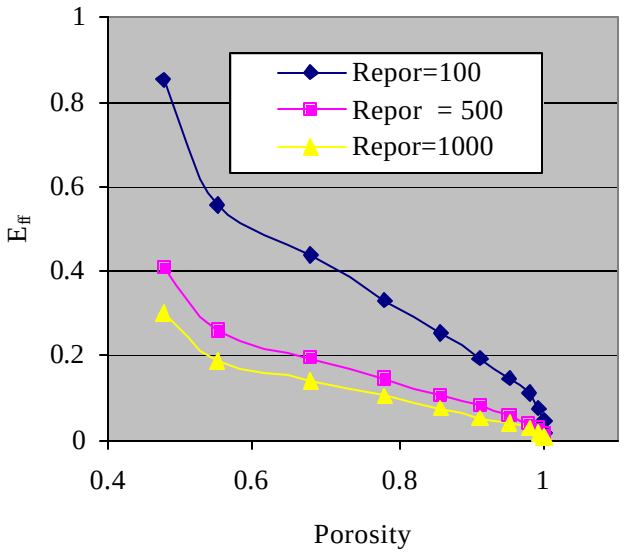

Fig. 2. Channel effective number versus porosity for flow across spherical beads.

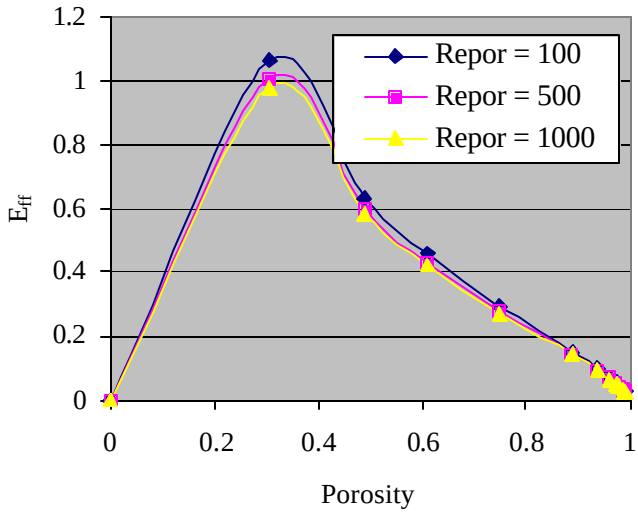

Fig. 3. Channel effective number versus porosity for flow across square tube banks.

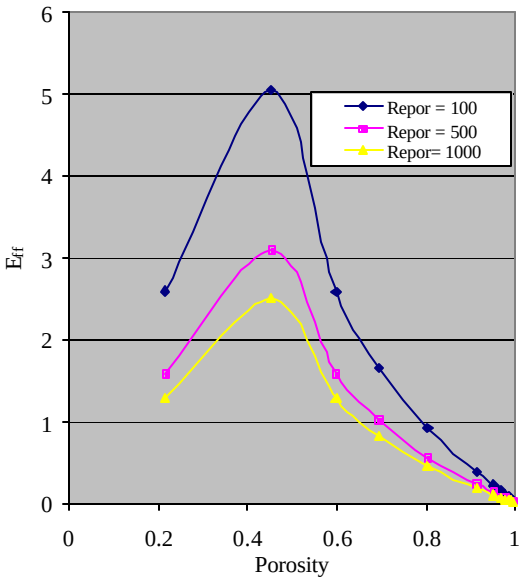

Fig. 4. Channel effective number versus porosity for flow across circular tube banks.

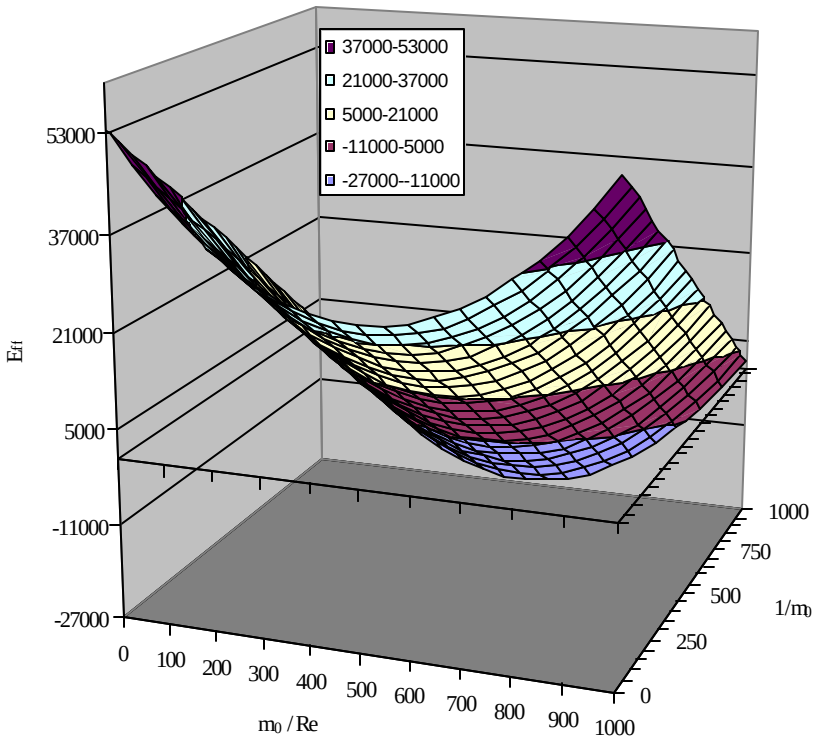

Fig. 5 Channel flow across circular tube banks optimization response surface

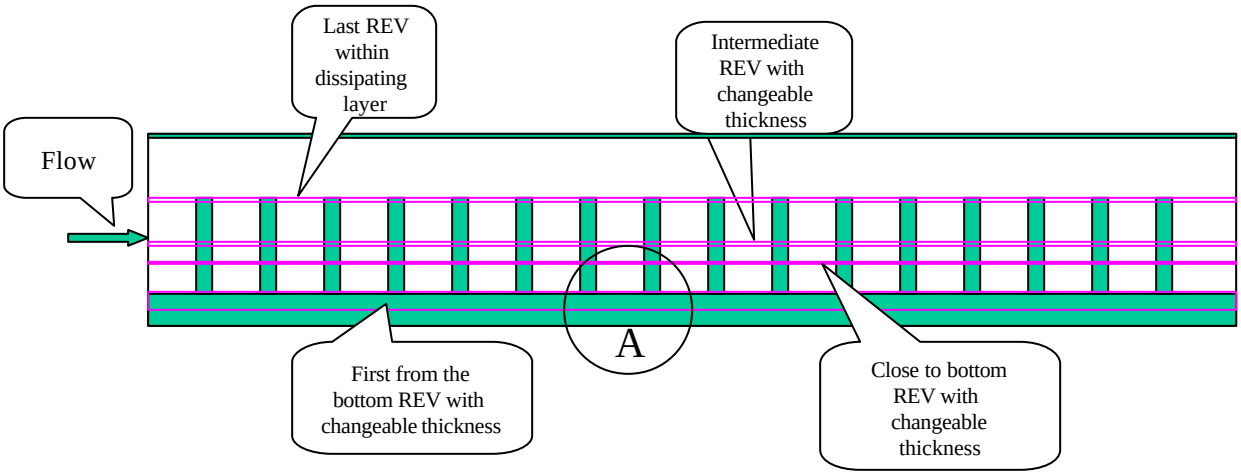

Fig. 6 a Flat Channel with Regular Heat Dissipation Layer

- in each phase averaging done separately

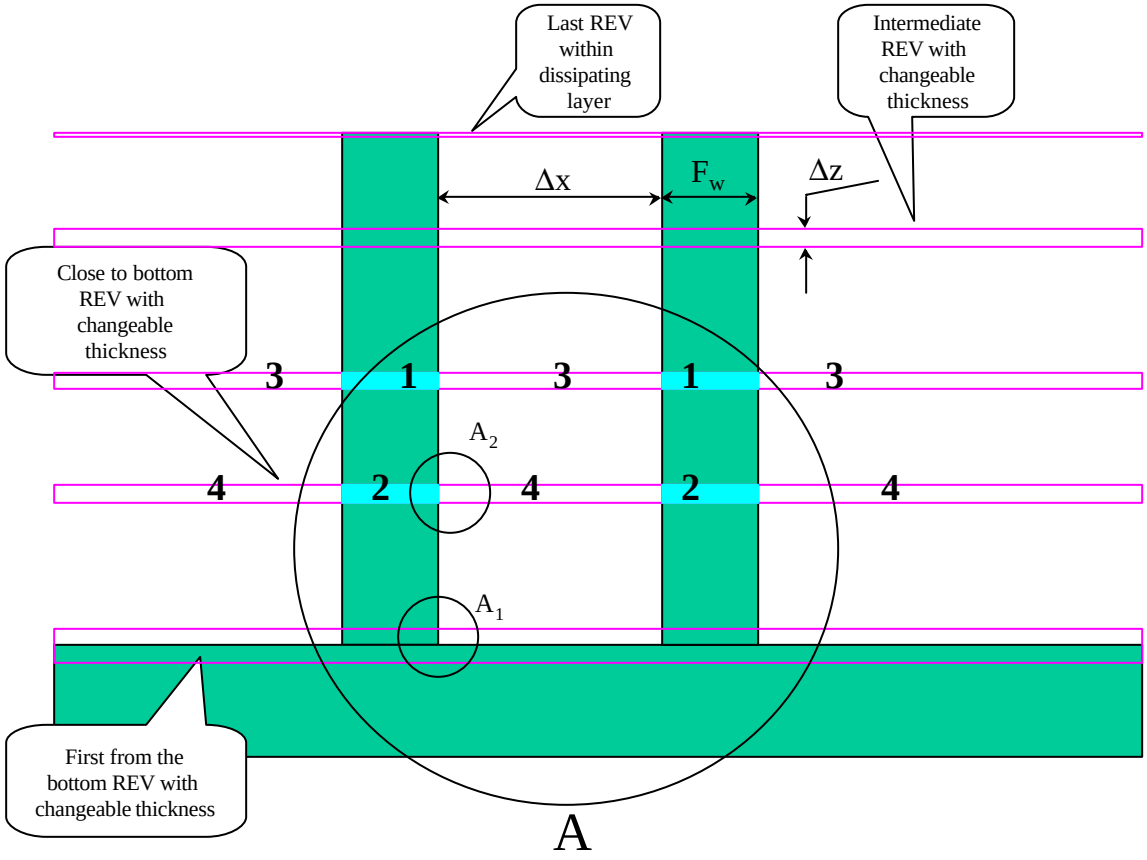

Fig. 6 b Solid phase temperature 1 and 2 and fluid phase 3 and 4 integrates in volumes separately for each REV and then represents point temperatures in the next scale of the problem